

Are rate sensitivity and strength effected by cross-slip in nano-twinned fcc metals

Robert J Asaro* and Yashashree Kulkarni

Department of Structural Engineering, University of California, San Diego La Jolla, CA 92093, United States

Received 28 May 2007; accepted 29 June 2007

Available online 4 December 2007

Synthesis of nano-twinned pure Cu by Lu et al. [L. Lu, R. Schwaiger, Z. W. Shan, M. Dao, K. Lu, S. Suresh, Nano-sized twins induce high rate sensitivity of flow stress in pure copper, *Acta Mater.* 53 (2005) 2169–2179] has produced materials with extremely attractive properties of combined high strength, strain rate sensitivity, and ductility adequate for applications. This note explores the underlying mechanistic reasons for this *via* a model analysis of dislocation interaction with nano-twinned boundaries. Interestingly, we find that processes like cross-slip, that lead to the absorption and transmission of slip through twin boundaries yet are normally associated with rate insensitive behavior, can lead to high strength and rate sensitivity as observed in experiment.

© 2007 Acta Materialia Inc. Published by Elsevier Ltd. All rights reserved.

Keywords: Nano-twins; Rate sensitivity; Activation volume

Nanocrystalline (nc) metals with grain sizes finer than 100 nm exhibit strength levels generally greater than 4–5 times those with grain sizes in the micron size range. The ductility of nanocrystalline metals is, however, typically just a few percent in uniaxial elongation (see *e.g.* Dao et al. [1]). Lu et al. [2,3], on the other hand, have shown that fcc metals (*viz.* Cu) processed to contain coherent twins with lamella thickness of the order of 20–100 nm display flow stresses of an order approaching, and in excess of, 1 GPa in tension and elongations to failure as high as 14%. In fact, the trends observed to date indicate that ductility as well as strength increase with decreasing twin lamella thickness. It follows, accordingly, that such attractive properties of nano-twinned metals has made them a focus of recent study. In particular, as the data display a strong sensitivity to strain rate it is of interest to understand what mechanisms mediate strength as well as induce such strong rate sensitivity. Here we use a simple model to explore potential underpinnings of such mechanisms and compare its findings to the recent atomistic simulations of Zhu et al. [4].

Data, such as presented by Lu et al. [2,3], analyzed to extract kinetic quantities such as the activation volume, V^* – a signature of the rate controlling processes – leads to the conclusion that

$$V^* = \sqrt{3}kT \frac{\partial \ln \dot{\epsilon}}{\partial \sigma} \quad (1)$$

is of order 10–20 b^3 , where b is the magnitude of a perfect Burgers vector. Eq. (1) implies that if $V^* = \alpha b^3$, and if \tilde{b} is measured in nanometers, then by a change in strain rate the flow stress changes by $\delta\sigma \approx 7/(\alpha \tilde{b}^3) \delta \ln \dot{\epsilon}$ MPa; analysis of the data of Lu et al. [2,3] suggests $10 \leq \alpha \leq 20$. It has been argued, moreover, that bulk dislocation activity is a vital component of plastic deformation in nano-twinned structures (see *e.g.* Zhu et al. [4] and Lu et al. [3]) as opposed, for example, to mechanisms such as grain boundary sliding which would involve activation volumes of order $v^* \sim 1 - 2b^3$ [5], and an associated strain rate sensitivity far greater than observed in experiment. Here we study the process of dislocation motion in nano-twinned structures for the purpose of uncovering the possible causes of the observed high strength and high rate sensitivity.

Figure 1b and c illustrate two types of processes of dislocation motion through a nano-twinned crystal; these processes are basically those simulated by Zhu et al. [4] (see their Fig. 1b) and involve slip transfer between two “bulk grains” and an intervening twin boundary. Figure 1b and c describe the processes of dislocation absorption and transmission onto and through a twin boundary. Figure 1a is taken from Asaro and Rice [6] and is used to analyze the steps depicted in Figure 1b and c. We note that two processes are possible. First is

* Corresponding author. Tel.: +1 858 534 6888; fax: +1 858 534 6373; e-mail: rasaro@ucsd.edu

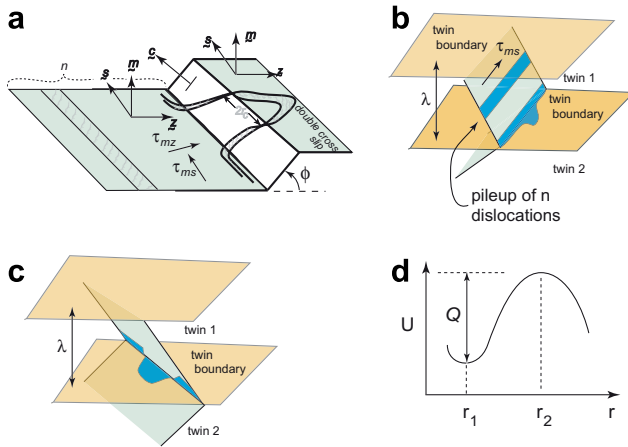


Figure 1. Models for slip transfer within a nano-twinned structure. (a) A basic model for the process of cross slip of a perfect fcc lattice dislocation, initially extended into two Shockley partials. Cross slip as envisioned here involves the constriction of the two partial dislocation, cross slip *via* a bowing out onto the cross slip plane, and extension on the cross slip plane. The figure actually illustrates a process of “double cross slip”. Note that the figure illustrates a pile up of n dislocations impinging on the site of the twin plane. (b) Process of cross slip of a dislocation from bulk crystal 1 onto the twin plane – the process of “absorption”. (c) Process of cross slip of the screw dislocation from bulk crystal 1 onto the slip plane in bulk crystal 2 – the process called “transmission”. (d) A schematic illustrating the energetics of the pathway of the cross slip process. Note the definition of the activation energy, $Q = U(r_2) - U(r_1)$ where r_2 is the “critical” bowed out radius of the transition (*i.e.* the saddle point) state.

the absorption of dislocations onto the twin boundaries (as in Fig. 1b). Second is the transmission of dislocations across the twin boundary and onto the slip planes in adjacent twin lamella (as in Fig. 1c). The absorption process would be followed by spreading of the absorbed dislocations on the twin plane causing it to shear; in this way the twin plane operates as a highly localized shear system as described by Dao, Kad and Asaro [7] for intermetallic TiAl lamella alloys. As dislocations accumulate on the twin boundaries, the boundaries “harden” thereby raising the flow stress generally and favoring transmission as opposed to further absorption. This hardening process is depicted in Figure 2 where the scenario shown involves the partials of a first dislocation absorbed onto the twin plane, $b_1^{(1)}, b_2^{(1)}$, spreading outward from point “o”, the intersection point of the slip plane of the first absorbed dislocation and the twin plane. A second extended dislocation (in red) gliding in one twin lamella approaches the twin boundary where its motion onto the twin boundary is inhibited by the first set of partial dislocations.

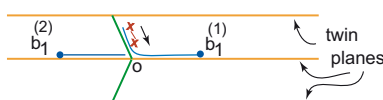


Figure 2. Model illustrating a first set of partial dislocations absorbing onto a twin boundary and spreading out on it thereby inducing “shearing” across the twin boundary plane. A second extended dislocation (in red) gliding in one twin lamella approaches the twin plane and its absorption is inhibited by the presence of the first set of partials. This causes a “hardening” of the twin plane.

The critical step analyzed by Asaro and Rice [6], involves the bowing process which, accordingly, is analyzed here. The model envisions an equilibrium dislocation pile up on the initial slip plane driven by the resolved shear stress τ_{ms} (see Fig. 1). Thus the number of piled up dislocations will scale as $n \sim \gamma \tau_{ms} \ell / Gb$ where G is shear modulus, ℓ is the slip line length, or in this case $\ell \sim \lambda$, the twin lamella thickness, and b is the magnitude of the Burgers vector. The coefficient γ depends on pile up geometry; for an isolated open ended pile up $\gamma = \pi$, but for a sequence of open ended pile ups spaced a distance p apart $\gamma = p/\ell$.

In the original Asaro and Rice [6] model (Fig. 1a), the cross slipping dislocation was assumed a perfect dislocation, initially extended into Shockley partials. In Figure 1b, however, the atomistic simulations of Zhu et al. [4] suggest that the critical process may instead involve the cross slipping (*via* a bowing process) of only the lead partial dislocation. There is, moreover, a geometric difference between the process of cross slip onto the twin plane (the absorption process) and cross slip onto the slip plane of the adjacent twin (the transmission process). This is that the angle ϕ is in the former case $\phi \approx +70^\circ$ whereas it is $\phi \approx -70^\circ$ in the latter. As noted below, this difference has rather obvious, yet significant, implications for the competitive interplay of the two processes, especially in a state of multi-axial stress.

The assumed activation pathway involves the spreading of a constricted dislocation segment along the intersection of the slip plane and the cross slip plane with energy U_c per unit length, and a bowed semicircular segment of radius r . The energetics of the activated pathway is sketched in Figure 1d. Traditionally, an activation volume would be defined as $v^* = -\partial Q / \partial \tau$ where τ is a “resolved shear stress”, but in cases as now considered it is clear that more than one component of stress is involved. In fact, a model like this clearly implies that $Q = Q(\tau_{ms}, \tau_{mz}, \tau_{zs})$ since τ_{mz} affects the process of constriction, and τ_{zs} directly contributes to the shear stress acting on the cross slip (or twin) plane as does τ_{ms} . That is, the simple concept of a Schmid rule is invalid here and the activation volume is more properly seen as a tensor, *viz.* with components formed as

$$v_{\alpha\beta}^* = -\frac{\partial Q}{\partial \tau_{\alpha\beta}}. \quad (2)$$

Asaro and Rice [6] assumed the lead dislocation bowed as a circular arc beginning from the rest radius r_0 . The energy of the semicircular arc was formed using the expression for the line tension of a circular loop as described by the first term in Eq. (3) (see Asaro and Rice [6]). The energy $U(r)$ as sketched in Figure 1d is thereby

$$U(r) = \Phi r \ln(r/r_0) - \mathcal{B}(r^{3/2} - r_0^{3/2}) + 2U_c r - \mathcal{E}(r^2 - r_0^2)$$

$$\Phi = Gb^2 \frac{2-\nu}{8(1-\nu)}, \quad \mathcal{B} = 1.4Kb \cos(\phi/2),$$

$$\mathcal{E} = \frac{1}{2} \pi \tau_{mz} b \sin(\phi).$$

(3)

K is the stress intensity factor at the head of the pile up, given as $K = \eta G n \tau_{ms} b$ where $\eta = 2, 1$ for an isolated open

ended pile up or sequence of open ended pile ups, respectively.

From Figure 1d the activation energy, Q , is defined as

$$Q = U(r_2, \Phi, \mathcal{B}, U_c, \mathcal{E}) - U(r_1, \Phi, \mathcal{B}, U_c, \mathcal{E})$$

$$U_c = 2E_{12} \ln(2E_{12}/\bar{\Gamma}r_0e) + \bar{\Gamma}r_0, \quad E_{12} = \frac{Gb^2}{32\pi}, \quad (4)$$

$$\bar{\Gamma} = \Gamma + \{\tau_{ms}b_s^{(z)} + \tau_{mz}b_z^{(2)}\},$$

which further exposes the inherent multiaxial stress dependence of the process.

The process as just described envisions a perfect dislocation undergoing the cross slip process, and it is this case we analyze first. After we rethink the events in light of Zhu et al.’s [4] simulation of the motion of an isolated screw dislocation and consider variations involving, *inter alia*, processes involving the bowing of just the lead partial dislocation.

A final note about the model adds needed perspective. Since the geometry of the critical process is prescribed, it is clear that it will likely not represent a true “minimum energy path”. Thus Q and $v_{\alpha\beta}^*$ are expected to be overestimated. Nonetheless, the value of the model rests in both in its simplicity and its generality and thereby in its ability to reveal important phenomenology such as the multi-axial stress dependence noted above.

To compute athermal stress levels required for critical bowing we require derivatives of Q when Q itself vanishes, *i.e.* we set both $\partial Q/\partial r = 0$ and $\partial^2 Q/\partial r^2 = 0$ at the transition state. Given that $\mathcal{E}r_0/\Phi \ll 1$ for representative stress levels (even in nc metals) we resolve these combined conditions by first defining $r_1 = er_0 \exp(-2U_c/\Phi) \approx er_0$, and then finding that $\mathcal{B} = (4\Phi/3r_1^{1/2}) [1 - \mathcal{E}r_1/\Phi]$. Then following Asaro and Rice [6] the athermal criteria for cross slip becomes to first order in the parameter $\mathcal{E}r_0/\Phi$

$$\tau_1 = 0.0071 \frac{(2-v)^2}{(1-v)^2} \times \frac{Gb}{r_1 \cos^2(\phi/2)} \left[1 - \frac{8\pi(1-v)\tau_{zs}r_1 \sin(\phi)}{(2-v)Gb} \right], \quad (5)$$

and where the latter approximation holds for representative values of U_c . We note that in Eq. (5) τ_1 is now defined as the net stress acting on the lead dislocation, that is for our two pile up models $\tau_1 = n\tau_{ms} = (\pi\tau_{ms}^2\ell/Gb, \tau_{ms}^2p/2Gb)$. For the case at hand for a fcc crystal where $\phi = \pm 70^\circ$ and taking $v = 1/3$ and $r_1 \approx er_0 \approx eb$ Eq. (5) is reduced to

$$\tau_1 \pm 0.65\tau_{zs} = 0.024G, \quad (6)$$

where the plus sign refers to absorption and the minus sign to transmission.

An immediate conclusion follows from Eq. (6), namely that when multi-axial states of stress prevail the processes of dislocation absorption or transmission are biased. Let $\tau_{ms} > 0$ and note that if $\text{sign}(\tau_{zs}) = \text{sign}(\tau_{ms})$, as is typically the case, then absorption is clearly favored over transmission. Moreover, with $\tau_1 = \pi\tau_{ms}^2\ell/Gb$ and ℓ associated with the twin lamella spacing, *i.e.* $\lambda = \ell$, Eq. (6) is plotted in Figure 3a and again in Figure 3c where τ_{ms}/G is plotted *vs.* $\lambda^{-1/2}$. For

the cases shown it was assumed that $\tau_{zs} = \tau_{ms}$. Thus the model naturally contains the scaling $\tau_{ms}^{\text{ath}} \propto \lambda^{-1/2}$ where “ath” refers to an athermal stress.

The data of Lu et al. [3] contains results from cases where $\lambda \approx 15$ nm and $\lambda \approx 100$ nm. For $\lambda \approx 15$ nm it appears that plastic flow commences when the tensile stress approaches $\sigma \approx 1$ GPa, at least at the largest strain rate they imposed. Figure 3a indicates that $\tau_{ms} \approx 350$ MPa for $\lambda \approx 15$ –20 nm; if the Taylor factor of 3.06 is used we estimate $\sigma \sim 3.06(350) \sim 1071$ MPa, in quite close agreement with the data. For the case of $\lambda \approx 15$ –20 nm, the predicted number of dislocations piled up at the twin boundary is of order $n \approx 2$, *i.e.* we forecast one additional dislocation behind the one actually cross slipping. This is important to note when comparing these model results to the atomistic simulations of Zhu et al. [4] who considered only the case of an isolated screw dislocation. At a somewhat reduced stress of $\tau_{ms} = 260$ MPa, we find that $n \approx 1$ in accord with Zhu et al.’s [4] simulations.

Consider now the case of a single screw dislocation cross slipping onto the twin plane. In Figure 3c we plot the energy $U(r)$ *vs.* r , where again $\tau_{zs} = \tau_{ms}$, but where now $\tau_{ms} = 252$ MPa. In fact we find that $Q \approx 0.44$ eV, is a value close to that found by Zhu et al. [4] in their numerical simulations for a case of a single screw dislocation cross slipping onto the twin plane. A caution is required here, however, since Zhu et al. [4] considered the case where the isolated screw dislocation was acted upon by only a resolved shear stress, *i.e.* only $\tau_{ms} \neq 0$.

The process is again analyzed for a perfect dislocation undergoing cross slip onto the twin plane, but in this case within a state of multi-axial loading. In particular, we set $\tau_{ms} = 260$ MPa and $\tau_{zs} = \eta\tau_{ms}$ with $0 \leq \eta \leq 1$. We compute the energy profile for an isolated perfect dislocation as shown undergoing cross slip onto the twin plane in Figure 3d. We make, however, several vital

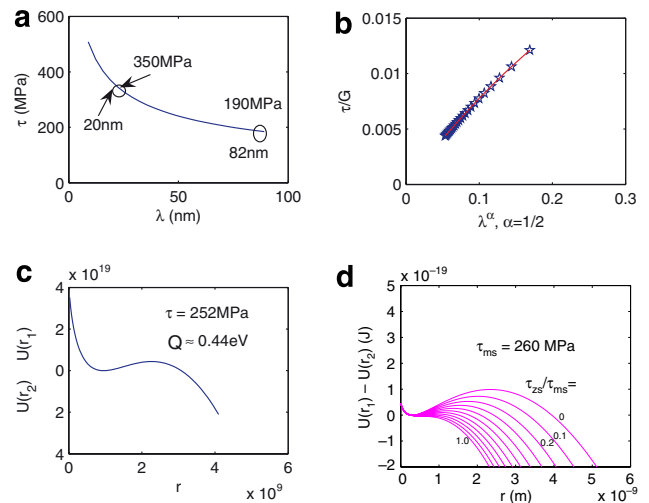


Figure 3. (a) τ_{ms} *vs.* λ , where $\lambda \approx \ell$ as taken herein, from Eq. (6). (b) τ_{ms}/G *vs.* $\lambda^{-1/2}$. For the cases shown it was assumed that $\tau_{zs} = \tau_{ms}$. (c) Energy pathway for a cross-slipping screw dislocation. (d) Energy profile for a perfect dislocation undergoing cross slip onto the twin plane. In this case the primary shear stress, τ_{ms} is set at $\tau_{ms} = 260$ MPa, $\phi = 70^\circ$, $n = 1$. Note the sensitivity of the energy profile and the resulting values of Q to the ratio of τ_{zs}/τ_{ms} .

changes to the original model, specifically concerned with the process of absorption onto a twin boundary. We first note that the requirement that the partial dislocations of the impinging perfect dislocation first coalesce is relaxed since glide onto the twin plane does not produce a stacking fault. This means that the lead partial dislocation bows itself and thus the Burgers vector appearing in the three terms listed below Eq. (3) become $b \leftarrow 1/\sqrt{3}b$, recognizing that the partial dislocation's Burgers vector is thus reduced. The sensitivity of the energy profiles with respect to the ratio τ_{zs}/τ_{ms} , and resulting estimated activation energy is revealed. In fact, when $\tau_{zs} = \tau_{ms}$, Q nearly vanishes. As it happens, and when $\tau_{zs} = 0$, $Q \rightarrow 0$ only as $\tau_{ms} \rightarrow 330$ MPa. This result is interesting since Zhu et al. report that the athermal stress computed in their simulations of this case is about 340 MPa. Also when $\tau_{zs} = 0$, as in the simulations of Zhu et al. [4], $Q = 0.62$ eV which is in reasonable accord with their computed value of $Q = 0.49$ eV for that case.

The activation volume v_{ms}^* is now estimated at $\tau_{zs} = 0$ to compare with the value $v_{ms}^* \approx 43b^3$ found by Zhu et al. [4]. When $\tau_{ms} = 260$ MPa, for example, we find that $v_{ms}^* \approx 135b^3$, a value much higher than reported by Zhu et al. [4] from their simulations. However, as τ_{zs} becomes an increasing fraction of τ_{ms} , the model predicts that v_{ms}^* decreases as expected. For example when $\tau_{zs} = 0.1\tau_{ms}$ and again where $\tau_{ms} = 260$ MPa, we find that $v_{ms}^* \approx 117b^3$; if $\tau_{zs} = 0.2\tau_{ms}$, $v_{ms}^* \approx 92b^3$, and so on. We also note that as τ_{ms} increases the activation volume decreases. For example when $\tau_{ms} = 268$ MPa and $\tau_{zs} = 0$, $v_{ms}^* \approx 117b^3$ and if $\tau_{zs} = 0.1\tau_{ms}$, $v_{ms}^* \approx 108b^3$, and so on. In fact, if $\tau_{ms} = 268$ MPa and $\tau_{zs} = 0.2\tau_{ms}$, $v_{ms}^* \approx 85b^3$. Thus the model predicts that under general states of multiaxial stress and at stress levels above, for instance, $\tau_{ms} \geq 270$ MPa the activation volume component $v_{ms}^* \rightarrow 50b^3$. Such numerical ranges of activation volume are consistent with the value $v_{ms}^* \approx 43b^3$ reported by Zhu et al. [4] although we need bear in mind that their simulations were carried out under a particular and simpler state of applied shear stress.

The effect of twin lamella thickness is complimentary to that just described for the general level of prevailing multi-axial stress. Clearly as λ decreases the applied stress levels required to cause dislocation absorption or transmission increases, in fact roughly as $\tau \propto \lambda^{-1/2}$ as shown in Figure 3. In the context of our model this leads to a decrease in n for a given stress level. For a case in point take, for instance, $\tau = 100$ MPa, and $\lambda \approx 100$ nm, in which case $n \approx 3$, and $\tau_{zs} = 0$. Then we find that $v_{ms}^* \approx 170b^3$. Now if $\tau_{ms} = 75$ MPa, and $\lambda \approx 180$ nm, $n \approx 4$, and again $\tau_{zs} = 0$, we find $v_{ms}^* \approx 600b^3$. Thus as λ increases, and in particular above 100 nm, and the athermal “yield stress” decreases, the activation volume increases to values that are typical of rate insensitive fcc metals.

To explore the tensorial nature of the activation volume we compute $v_{zs}^* = -(\partial Q / \partial \tau_{zs})_{\tau}$ where the subscript τ indicates holding all other components of stress con-

stant. An estimate from the curves shown in Figure 3d is that $v_{zs}^* \approx 26b^3$, which reveals that the process of cross slip onto the twin plane is indeed expected to produce a sensitivity to strain rate as observed in experiment. In fact, this value is nearly a factor of 2 smaller than the value for $v_{ms}^* \approx 43b^3$ reported by Zhu et al. [4] for this case.

Since the basic process of dislocation absorption and transmission considered here are variants of the cross slip process depicted in Figure 1a, it is necessary to account for the apparent conflict between the rather low value of activation volumes found by using our model for nc crystals and those normally reported for cross slip in fcc crystals. For example, Krauz and Eyring [5] list values for activation volume in the range $v^* \sim 100\text{--}1000b^3$ for cross slip, a range consistent with the fact that fcc crystals are rather rate insensitive! Resolution of this comes *via* several pathways. For one, and as already noted, the predicted activation energies and volumes are quite sensitive to both stress state and to stress magnitude. At stress levels typical of fcc metals containing micron size grains we would find, as noted above, that $v^* > 100b^3$ and in fact lies in the range $100b^3 < v^* < 1000b^3$. But when the prevailing stress levels are, say in the range where $\tau_{ms} > 270$ MPa for example, the activation volumes are reduced to well below $100b^3$ as demonstrated in the various examples described above. Grain size, or in the present case twin lamella thickness, has a complimentary affect. If $\lambda < 100$ nm and, in the context of our model, $n \leq 2$ then the prevailing stress levels are in the requisite range where $v^* < 100b^3$. It would be of value to explore these trends *via* the sort of atomistic simulations reported on by Zhu et al. [4].

As far as comparison with experiment, we note that by using a Taylor-like picture for making a transition from “single crystal” behavior to polycrystalline response we would estimate the activation volume V^* in Eq. (1) as $V^* \approx (\sqrt{3}/M)v^*$, where $M = 3.06$ is Taylor's factor. Thus if $v^* \approx 50b^3$, then $V^* \approx 28b^3$. Thus the present model provides a nearly consistent picture for the experimentally observed increase in rate sensitivity and concomitant decrease in activation volume with decreasing twin lamella thickness below say 100 nm.

- [1] M. Dao, L. Lu, R.J. Asaro, J.T. M Hosson, E. Ma, Acta Mater. 55 (2007) 4041–4065.
- [2] L. Lu, Y.F. Shen, X.H. Chen, L.H. Qian, K. Lu, Science 304 (2004) 422–429.
- [3] L. Lu, R. Schwaiger, Z.W. Shan, M. Dao, K. Lu, S. Suresh, Acta Mater. 53 (2005) 2169–2179.
- [4] T. Zhu, J. Li, A. Samanta, H.G. Kim, S. Suresh, PNAS 104 (2007) 3031–3036.
- [5] A.S. Krausz, H. Eyring, Deformation Kinetics, J. Wiley, New York, 1975.
- [6] R.J. Asaro, J.R. Rice, J. Mech. Phys. Solids 25 (1977) 309–338.
- [7] M. Dao, B. Kad, R.J. Asaro, Philos. Mag. A 75–2 (1997) 443–459.